Journal of Mining and Environment (JME) Vol. 18, No. 4, 2026, 1307-1323

Shahrood University of Technology

Journal of Mining and Environment (JME)

Journal homepage: www.jme.shahroodut.ac.ir

Iranian Society of Mining Engineering (IRSME)

Evaluation of Rock Characteristics and Degradation Induced by Cyclic Freezing-Thawing Action of some Igneous Rocks under Climate Change Conditions in Saint Katherine Arid Mountain Region, South Sinai, Egypt

B.G. Mousa[1,2*], Marzouk Mohamed Aly Abdelhamid[2], Mohamed Elgharib Gomah[2], M. M. Zaki[2], H.A. Farag[2], W.M. Draz[2], Remonda Damian[1,3,4], and Yousef A. Al-Masnay[1,3]

1. State Key Laboratory of Ecological Safety and Sustainable Development in Arid Lands, Xinjiang Institute of Ecology and Geography, Chinese Academy of Science, Urumqi 830011, China
2. Department of Mining and Petroleum Engineering, Faculty of Engineering, Al-Azhar University, Cairo 11884, Egypt
3. University of Chinese Academy of Sciences, Beijing 100049, China
4. Soils and Water Use Department, Agricultural and Biological Research Institute, National Research Center, Cairo, 12622, Egypt

Article Info

Received 6 February 2026
Received in Revised form 30 May 2026
Accepted 31 July 2026
Published online 31 July 2026

DOI: 10.22044/jme.2026.17427.3461

Keywords

Igneous rocks
Physical weathering
Freezing-thawing
Deterioration function model
Long-term durability

Abstract

Rock damage due to severe environmental conditions may affect durability over time. Therefore, this study aims to investigate the degradation of igneous rocks triggered by freezing-thawing weathering and to predict their loss of integrity. Four types of igneous rocks were collected from the Saint Katherine mountain area, Sinai, Egypt, and subjected to 100 cycles of the freeze-thaw method. The land surface temperature variation was analyzed using remote sensing data as an indicator for selecting the freeze-thaw temperature for our experiments. The physical and mechanical characteristics of the studied rocks, such as dry bulk density, effective porosity, ultrasound pulse velocity, abrasion loss, unconfined compressive strength, and point load strength, were measured after 0, 20, 40, 60, 80, and 100 cycles of the freeze-thaw process and evaluated using deterioration ratios and statistical models. Exponential and linear decay function models were established to statistically assess the integrity loss rate of the mechanical strength properties of the selected rocks. Two critical factors, decay constant and half-life, were derived from the studied models and used to predict rock durability. This evaluation suggests that the behavior of rock decay is very similar across different types of igneous rocks, exhibiting a strong correlation and high precision. Therefore, these models are reliable and valid for predicting the durability of the studied igneous rocks. Results also showed that the tested igneous rocks can be used as construction stones in regions exposed to repeated cyclic freezing-thawing weathering and harsh environmental conditions over long periods without disintegration.

1. Introduction

Igneous rocks of variable shapes, patterns, colors, and chemical constituents are plentiful in north, central, and south Sinai areas of the Eastern Desert [1–6]. Egypt takes the seventh ranking in the production of building or decorative stone throughout the world [7–10]. These stones are commonly used as building or ornamentals stones for cladding, paving and flooring construction purposes because of their high diversity and great resistance and durability [11–14]. Due to numerous outdoor applications, it is necessary to understand that any construction stones used will change in appearance and exposed to some damage as an unavoidable consequence of disintegration due to long-term weather influences. Most rocks used as construction or decorative stones subjected to long-term severe climatic conditions tend to degrade. These processes, named as rock damage,

Corresponding author: dr.bahaa1@azhar.edu.eg (B. G. Mousa)

weathering and disintegration, indicate an altered state of the construction stone [15]. Freezing-thawing is a major physical weathering process which occurs in humid weather wherein the temperature recurrently fluctuates over and under freeze point [16, 17]. When water transforms to ice, it increases in size by up to 9% and generating overstresses into the micro-pores and cracks. When the compression exceeds the stone's tensile strength, fresh micro-fractures are developed and the existent ones are expanded, thus these variations can reduce the strength and durability of rocks [18–22]. Zhang et al. [23] observed that there were more inside pores as the number of cyclic freezing–thawing increments, because of the growth of fresh micro-cracks and the widening of the main pores. Moreover, Zhang et al. [24] indicated that the combined temperature and pressure fields induced by cyclic freezing–thawing cycles degrade the physico-mechanical characteristics of rock masses, which indirectly cause geo-hazards, including landslides and damage. Ruedrich et al. [25] found that obvious damage cannot be identified in most conditions till 50 cycles of weathering processes have been completed. Martínez et al. [26] indicated that the freezing–thawing is a non-linear process wherein long times of clear constancy are accompanied by a prompt and catastrophic damage. Consequently, the principal tests performed on a definite number of cyclic frost weathering do not consider the variety of freezing–thawing aging of stones. Bayram [27] indicated that natural rocks in cold areas were exposed to the freezing-thawing weathering process at least once a year.

The influence of frost aging process on the engineering parameters of rocks has been investigated in several studies [28–33]. Mutluturk et al. [34] suggested a decay function approach for predicting the damage rate of rocks against the cyclic freezing–thawing, but this model used only Shore hardness method and other mechanical strength parameters are ignored. Yavuz et al. [35] developed a model formula to estimate the indicator parameters of damaged carbonation rocks against freezing–thawing cycles and indicated that the loss in index property of a damaged stone based on its main engineering property and porosity with regard to the coefficients for a distinctive index property. Tan et al. [36] performed the unconfined and tri-axial compression tests on granitic rocks subjected to freezing–thawing weathering process in order to predict the deterioration rate. Liu et al. [37] indicated the degradation of the main laws of frost weathering and the variation trend of physico-mechanical characteristics of granite and andesite rocks against the cyclic freezing–thawing depending on the environmental conditions and the temperature variations in the Qinghai-Tibet Plateau. Ozbek [38] evaluated the physico-mechanical parameters of ignimbrites of different colors from Central Anatolia against the impact of freeze–thaw cycles. He indicated that such cycles had a clear influence on engineering characteristics of the stones. Jamshidi et al. [39] determined the durability of 14 different types of construction stones under freeze–thaw cycles. Jamshidi et al. [40] evaluated the effect of cyclic frost aging process on the mechanical parameters of travertine rock specimens depending on half-life and decay constant parameters. Momeni et al. [41] indicated the variations in engineering characteristics of Aluand granitoid stones in Iran after 300 cyclic freezing-thawing. Zhang et al. [42] attempted to estimate the results of subjecting sandstone rocks to freeze–thaw cycles and chemical weathering using the decay function approach. Ma et al. [43] investigated the influences of the cyclic freeze–thaw on the dynamic strength and energy allocation of stones. They proved that the dynamic characteristics reduced with increasing cycles number. Fan et al. [44] evaluated the impacts of freezing-thawing on the engineering parameters and elastic property of dry and saturated sandstone rocks. Chen et al. [45] evaluated the mechanical behavior and damage of granitic rock samples under freeze–thaw cycles. They concluded that there are three damage parameters with various definitions including modulus of elasticity, density, and porosity that can precisely describe the degree of deterioration for granitic rocks against the cyclic freeze–thaw weathering. Yun et al. [46] established a fatigue damage constitutive model for fractured granitic rock specimens, including main fracture deterioration, freezing–thawing weathering, and load deterioration and proved that this model valid for the combined influences of freezing–thawing cycles and fatigue load on granitic specimens.

Although several studies have applied exponential decay models to quantify freeze–thaw deterioration in rocks, no such model has yet been calibrated for the igneous rock types in our study area. Moreover, the integrity loss rates of these specific rocks under freeze–thaw action remain unquantified. Therefore, the main contributions of this work are: (i) an initial assessment of the physico-mechanical deterioration of the study area's igneous rocks under laboratory freeze–thaw cycles, (ii) the application of a statistical decay function model to estimate their durability and integrity loss, and (iii) the use of remote sensing-derived land surface temperature data to define cycle conditions that reflect local real-world thermal regimes. Accordingly, this research will investigate the degradation of the engineering properties of selected igneous stones subjected to repeated freeze–thaw weathering and will statistically predict their durability using a degradation ratio and decay function model, with experimental temperatures informed by remote sensing analysis.

2. Materials and Methods

2.1. Materials

In this paper, four different kinds of igneous stones, such as Red Granite (GR), Granodiorite (GD), Diorite (DI), and Monzonite (MO), were collected from the Saint Catherine area, South Sinai Peninsula, Egypt, and are located between longitudes 33° 57' East and latitudes 28° 33' North (Figure 1a). All of them are used locally as construction and ornamental stones. The peninsula has the maximum variation in altitude of any area within Egypt, ranging from low-lying coastal plains to high mountains, with the highest peak being Mount Catherine. The area consists of steep mountains intersected by deep canyons such as wadis, providing largely high mountains composed of magmatic and/or igneous rocks [47]. The elevation increases from northeast to southwest and ranges from 805 to 2,247 meters (Figure 1c). Figure 1b shows the average land surface temperature variation in the Saint Catherine region during the last years (2015–2025). It is observed that the temperature decreases from northeast to southwest (i.e., the lowest temperatures occur at high mountains). The studied igneous rock specimens were extracted from large blocks measuring 50 × 50 × 50 cm³ and prepared in cubical and cylindrical shapes. The selection of rock samples was free from fissures or micro-cracks to avoid the influence of anisotropy on the measurements. Two sets of tested igneous rock samples were examined in this paper: the first set was used to determine the main physico-mechanical properties (unweathered specimens), while the other samples were exposed to freezing-thawing cycles. The relationships between physico-mechanical parameters were investigated after every 20 cycles of weathering, up to 100 cycles. The results obtained were statistically analyzed using degradation ratio and mathematical exponential and linear decay function models to evaluate long-term durability and potential integrity loss characteristics.

2.2. Methods

2.2.1. Mineralogical and chemical analysis

Performing mineralogical and chemical analyses is a useful tool in assessing rock characteristics and their resistance to weathering [48]. Hence, in this study, X-ray diffraction (XRD) was performed to determine the mineralogical composition of the studied rocks. Representative specimens of igneous rocks were selected for XRD analysis. For each rock type, a small amount of igneous rock sample was finely crushed and prepared for XRD analysis. This analysis revealed that the studied igneous rock samples are composed of quartz and feldspars as secondary minerals, associated with some mafic minerals including biotite and hornblende as accessory minerals (Table 1). It was also observed that the tested rock samples of granite (GR) contain the highest percentage of quartz (25.18%), while the lowest percentage (11.32%) was found in rock specimens of diorite (DI). Additionally, it was found that diorite rock samples recorded the highest percentage of mafic minerals (24.20%). The XRD pattern for the tested igneous rocks is presented in Table 1. Polarized optical microscopy (POM) was also used to determine the petrographic and textural characteristics of the igneous rocks. The results of this analysis are shown in Table 2. Furthermore, in this study, X-ray fluorescence (XRF) was performed to determine the chemical composition. Representative samples were analyzed to obtain the mean percentage of major element oxides (w.t%) (Table 3).

Table 1. Mineralogical composition of the studied igneous rocks (Granite, GR; Granodiorite, GD; Diorite, DI; Monzonite, MO). Abbreviations: Q = Quartz, AF = Alkali feldspars, PL = Plagioclase feldspars, H = Hornblende, BI = Biotite.

Rock type	Q(%)	AF(%)	PF(%)	H(%)	B(%)	Accessories(%)	Mafics(%)
Granite (GR)	25.18	41.37	21.22	6.03	5.15	1.08	11.18
Granodiorite (GD)	20.33	17.32	49.60	6.11	4.95	2.66	11.06
Diorite (DI)	12.32	6.95	61.07	14.66	4.14	1.02	18.80
Monzonite (MO)	19.61	40.44	27.33	3.14	6.87	2.10	10.01

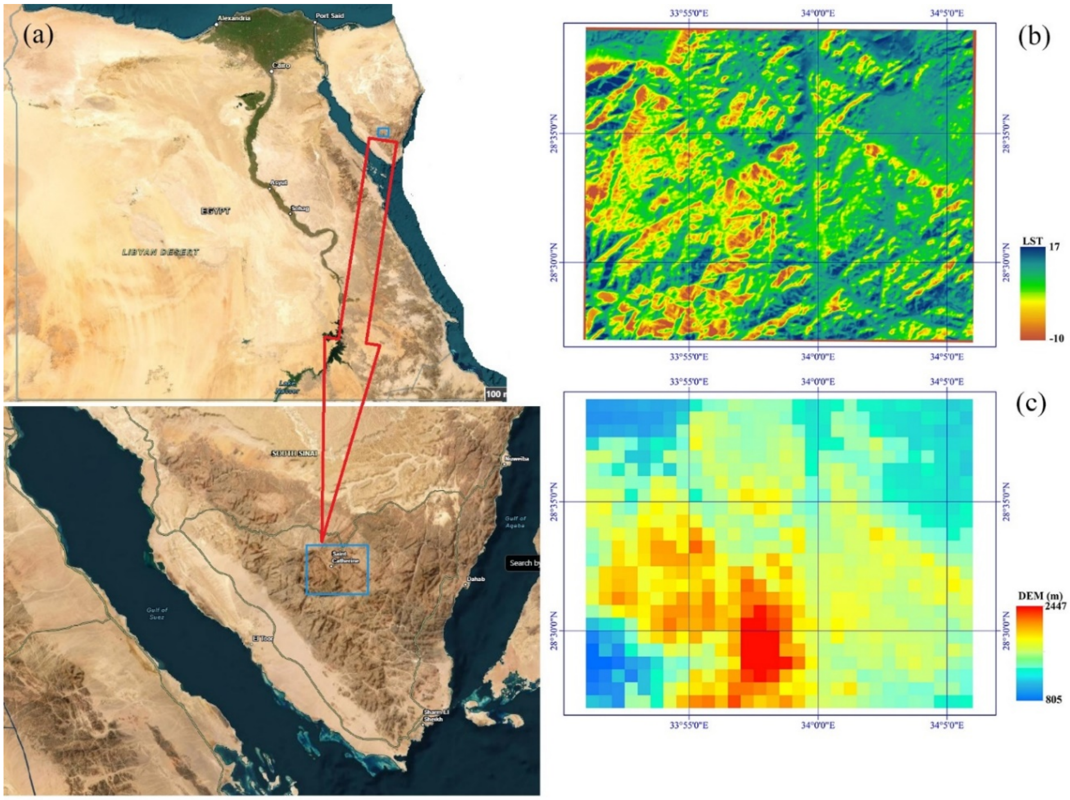

Figure 1. (a) Location map of the study area. (b) Average surface temperature variation during the winter season over the period 2015–2025. (c) Elevation variation across the arid landscape of Saint Katherine.

Table 2. Petrographic properties of studied igneous rocks.

Rock type	Code	Description
Granite	GR	Coarse-grained in texture (>4mm) and quartz frequently reacts with the alkali feldspars forming graphic texture at their boundaries. Secondary albitization is also observed in this type of granite.
Granodiorite	GD	Medium grains (2-4mm), holo-crystalline and non-porphyritic and equigranular in texture. Quartz occur as medium grains and filling space between the other main mineral constituents in this type of rock.
Diorite	DI	Medium to coarse grains, homogeneous and indicating strong intergranular texture. Plagioclase is the most dominant mineral in the diorite rocks and quartz fills the interstitial space between the other main constituents.
Monzonite	MO	Coarse grains and indicating perthitic texture. Perthitic intergrowths are often prevalent forming a patchy kind. Medium blobs of magnetite are observed in these samples.

Table 3. Chemical analysis of the tested igneous rocks. LOI = Loss on ignition

Rock type	SiO_2 (%)	CaO	MgO	K_2O	Na_2O	Al_2O_3	Fe_2O_3	LOI	Total
Granite (GR)	69.03	1.09	1.56	3.95	4.02	14.99	3.90	2.67	99.21
Granodiorite (GD)	63.71	1.64	3.25	4.00	3.87	15.83	4.27	3.60	100.17
Diorite (DI)	57.44	2.16	4.51	4.86	4.33	17.75	3.82	4.71	99.58
Monzonite (MO)	62.89	2.34	4.17	3.65	3.44	14.02	5.73	3.43	99.68

2.2.2. Physical and mechanical characterization

Weathering processes affect the physico-mechanical properties of rocks used as construction or decorative stones and cause deterioration problems. These characteristics are studied through the laboratory tests used for the investigation of the igneous rock specimens.

2.2.2.1. Physical characteristics

Physical properties are the crucial indexes to determine the stone durability. The presence of water affects the stone properties and causes deterioration [49]. In this study, the physical parameters including the bulk density, water absorption by weight, and the effective porosity were determined for physical characterization of the tested igneous rock specimens. Additionally, in this study, a non-destructive methods including the ultrasonic pulse system was also carried out to estimate the long term durability of the studied rocks specimens. The physical properties were determined using the saturation technique outlined by ISRM [50]. For this reason, oven-dry weight, saturate weight and volume of specimens were determined then dry density, water absorption and effective porosity were calculated through Equations 1, 2 and 3, respectively: six specimens were tested for every rock type and their average values were determined.

$$Bulk\ density = \frac{dry\ weight}{Volume} \tag{1}$$

$$Absorption\ of\ water = \left(\frac{saturate\ weight - dry\ weight}{dry\ weight}\right) \times 100 \tag{2}$$

$$Effective\ porosity = \frac{saturate\ weight - dry\ weight}{water\ density \times Volume} \times 100 \tag{3}$$

2.2.2.1.1. Ultrasonic system

The pulse transmission method was used to determine the velocities of the longitudinal waves. Therefore, in this paper, an ultrasound detector device couples two piezoelectric sensors on the opposite faces of the specimen transducers. The frequency was 1 MHz. Cylindrical rock specimens with a radius of 2.5 cm were prepared, and the ratio of height to diameter was two, based on the procedures proposed by Martinez-Martinez et al. [51]. A grease material was applied to the flat surface of the specimen. The specimen was placed between the transmitter and the receiver, and the transducer faces were firmly pressed against the sample faces until a stable velocity was displayed. The ultrasound pulse velocity (V_P) was obtained from the ratio of the path length (cm) of the samples to the interval duration (μs) from the generator to the receiver at the opposite end. Six specimens of each rock type were used for this test, and their average value was calculated.

2.2.2.2. Mechanical characteristics

The mechanical characteristics such as uniaxial compressive strength, point load strengths, and the abrasion loss were investigated for characterization of studied specimens, and assessing the long term deterioration of rock specimens.

2.2.2.2.1. Uniaxial compression test

The uniaxial compressive strength (UCS) of rocks is a crucial property for choosing rocks used as construction or dimension stones in addition to predicting the rock durability under aggressive climatic conditions [52]. The uniaxial compression test was performed on cubical samples of 10×10×10 cm^3 according to the test methods outlined by the standard [50]. In this paper, a self-designed microcomputer electro-hydraulic system was used. The maximum capacity was 1000 KN with loading compression rate between 0.1 and 0.20 KN/s with a ±1% precision. The sample surfaces on opposite sides were regularized and vertical to the axis of the rock sample. Consequently, the force should be distributed regularly. The direction of loading has been done from bottom to top. Seven samples for each igneous rock type were tested and the average value was recorded.

2.2.2.2.2. Point load test

Point load index test (IS), as one of the significant mechanical methods was done in this study. It is a widely an in-direct method used for determining the rock strength because it's easy, simple in addition the simplest of sample preparation. The employ of point load test for estimating durability of rock used for ornamental purposes. The point load strength was carried out according to the test methods procedures outlined by ISRM [53]. Axial testing methods were applied in this study on a diametrical specimens of 5 cm and the ratio between length and diameter equals to 0.8. For every rock type, the number of samples was seven and the average values were attained.

2.2.2.2.3. Abrasion test

The prepared and tested igneous rock specimens were based on the procedures outlined by [54, 55]. The cross sectional area of the tested samples was 7 x 7 cm^2. The rock specimen was fixed in the holders and rotated 352 revolutions at a speed of 38 rpm. Quartz sand was used as an brasive substance at feed rate of 750 g for each test. Abrasion test procedures were performed according to the Egyptian Code [56]. During this method, the machine rotated a grinding wheel whereas the specimen was fixed and exposed to constant force of 5 kg. The sample weight was recorded prior to and after test. The abrasion decrease was attained from the following equation [57]:

$$Abr = \left(\frac{w_1 - w_2}{\rho \times a}\right) \quad (4)$$

Where, Abr is the abrasion loss (mm), W_1 is the weight of the sample prior to the test (g), W_2 is the weight of the sample after abrasion (g), ρ is the density (g/cm³), and a is the cross-sectional area (cm²).

2.2.3. Freezing–thawing test

To evaluate the durability of the tested rock specimens, they were subjected to freeze–thaw (F-T) cycles up to 100 cycles following established procedures [58,59]. First, the prepared rock specimens were oven-dried at 105 °C for 48 h until the mass change was less than 0.1%. After cooling to room temperature (20 °C), the specimens were weighed. Second, to achieve full saturation, the dried specimens were placed in a vacuum desiccator and saturated with distilled water at 20 °C under a vacuum pressure of 6 kPa for 4 h, followed by 24 h immersion at atmospheric pressure. Third, the saturated specimens were placed in a deep freezer pre-cooled to −15 °C and frozen for 12 h. Finally, the specimens were removed from the freezer and immersed in distilled water at 20 °C for 12 h (Figure 2). Each complete cycle thus lasted 24 h (12 h freeze, 12 h thaw). The temperature range (−15 °C to +20 °C) was selected based on land surface temperature (LST) data from the study area (Saint Catherine, Sinai): MODIS LST records (2015–2025) (Figure. 1b) show winter minimum values of −10 °C and winter daytime maximum values of +17 °C. The laboratory range was extended slightly to accelerate testing while preserving the freeze–thaw damage mechanism and ensuring a safety margin beyond local extremes. Physico-mechanical properties, including dry density, effective porosity, ultrasound wave velocity, uniaxial compressive strength, point load index, and abrasion resistance, were measured every 20 cycles (i.e., at 0, 20, 40, 60, 80, and 100 cycles).

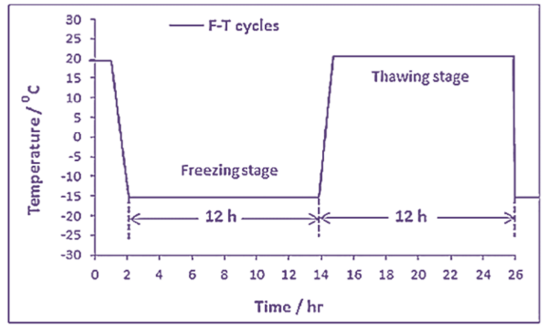

Figure 2. Temperature–time changes schematic diagram of a freezing-thawing process.

2.2.4. Mathematical modeling

2.2.4.1. Deterioration function model

Despite many previous studies on various aspects of the influence of freezing-thawing on rocks, which have been conducted over different decades, numerical methods are not sufficient for predicting the loss of rock integrity under the freezing-thawing weathering process. Therefore, in this study, a mathematical decay function model can be determined through simple regression analysis, including exponential and linear regressions. These models were developed and verified using mechanical tests such as uniaxial compressive strength and point load index strength. Two significant parameters are derived from this model to predict the decrease in mechanical strength properties and the degradation rate under cyclic freezing-thawing. These parameters can save time in predicting the characteristics of integrity loss and the lifespan of stones as durable structures. After the cyclic freezing-thawing process, the decay rate of the tested rock samples was evaluated using the damage function model. Mutluturk et al. [34] proposed a damage function model employing a decay constant (λ) and half-life ($N_{1/2}$) parameters to assess the loss of rock integrity in various rock specimens due to freeze-thaw and heat–cool weathering. The statistical model suggests that the integrity loss rate induced by weathering actions is proportional to the stone integrity at the beginning of each cycle (Equation 5):

$$-(dI/dN) = \lambda I \quad (5)$$

Where (dI/dN) is the rate of deterioration, λ is the decay constant, I is the rock integrity and N is the cycles numbers. The minus sign in Eq. 5 indicates the rock integrity loss is decreasing. By integrating Eq. 5, between the initial rock integrity (I0) and the integrity after N cycles (IN), we obtain an equation in logarithmic form as the following:

$$\int_{I0}^{IN} (dI/dN) = \lambda I \rightarrow ln\left(\frac{I0}{IN}\right) = \lambda N \quad (6)$$

Equation 6 can be expressed in exponential form as follows:

$$\boldsymbol{IN} = I0e^{-\lambda N} \quad (7)$$

The term $e^{-\lambda N}$ is the decay factor, which illustrates the rate of the residual integrity after N cycles, i.e. (I_N /I_0). In addition, the decay constant (λ) parameter illustrates the average relative decrease of integrity at any single cycle and it can be used to measure the durability of stone, the half-life ($N_{1/2}$) parameter shows the number of cycles required to reduce the rock integrity to its half value. This parameter is inversely proportional to the decay constant. By substituting (I_0/2) with I_N in Equation 7, the half-life ($N_{1/2}$) can be determined shown in Equation 8 (Altindag et al. 2004):

$$N_{1/2} = ln2/\lambda = 0.6930/\lambda \quad (8)$$

The decay function model can also be expressed as a linear regression model. The general form of the decay function model is given by the following linear regression equation:

$$IN = -\lambda N + I0 \quad (9)$$

Similarly, by replacing (**I_0/2**) with **IN** in Equation 9, the half-life (**$N_{1/2}$**) can also be obtained as shown in Equation 10:

$$N1/2 = I0/2\lambda \quad (10)$$

The output parameters can provide significant information for the rendering of rocks against freezing-thawing tests when the model is applicable for their integrity. This can help in decision-making in many daily applications.

3 Results and Discussions

The degradation of rocks induced by weathering tests is a function of their physico-mechanical properties. Consequently, the determination of these characteristics is crucial for evaluating durability. The average values of the initial engineering properties and standard deviations of the tested igneous rocks (untreated specimens) are presented in Table 4. Among the tested igneous rocks, the diorite samples (DI) have the highest dry density, and the monzonite rock specimens (MO) have the lowest density. This variation is attributed to their mineralogical composition and the high percentage of heavy minerals or mafics, including hornblende and biotite, in the diorite samples. The lowest and highest values of water absorption, effective porosity, and ultrasound pulse velocity were observed in rock samples of diorite and monzonite, respectively. This indicates that ultrasound pulse velocity depends on water absorption and effective porosity. This relationship was also observed in mechanical characteristics. Table 4 shows the highest uniaxial compressive and point load strengths of 162.21 MPa and 10.12 MPa for diorite specimens, compared to the lowest values of 99.97 MPa and 7.12 MPa for monzonite specimens. Additionally, diorite samples exhibit the minimum abrasion loss rate (0.10 mm), while monzonite samples show the maximum abrasion loss (0.19 mm). Quantitatively, the higher hornblende content (14.66%) and strong interlocking in diorite directly correlate with its lower porosity and higher strength, whereas the higher biotite (6.87%) and magnetite content in monzonite correlate with its faster deterioration [60]. Tests have shown that hornblende-rich rocks have higher strength than magnetite-rich rocks. This difference is attributed to their mineralogical and textural characteristics and the presence of a high percentage of weak or weathered minerals such as biotite (6.87%) in the monzonite sample. It was also observed that monzonite specimens contain medium-sized magnetite blobs, which lead to a reduction in strength properties.

Table 4. Mean values and standard deviations of physico-mechanical characteristics for unweathered specimens: ρb (dry bulk density), W (water absorption), pe (porosity), UCS (uniaxial compressive strength), IS (point load strength index), Abr (abrasion loss), Vp (ultrasound pulse velocity).

Rock type	ρ_b (g/cm^3)	W (%)	p_e (%)	V_p (Km/s)	UCS (MPa)	IS (MPa)	Abr (mm)
GR	2.57±0.02	0.32±0.34	0.90±0.66	4.64±0.33	117.32±1.84	8.04±0.75	0.15±0.33
GD	2.65±0.14	0.26±0.21	0.86±0.52	4.84±0.87	132.95±1.31	8.96±0.32	0.14±0.44
DI	2.76±0.05	0.24±0.40	0.79±0.50	5.64±0.72	162.21±1.83	10.12±0.60	0.10±0.66
MO	2.62±0.07	0.46±0.27	1.12±0.80	4.02±0.98	99.97±1.89	7.12±0.37	0.19±0.60

3.1. Impact of freeze-thaw cycles on physico-mechanical properties

The engineering characteristics of the studied rocks during freezing-thawing cycles are displayed in Table 5. To evaluate the influence of freezing and thawing on the engineering characteristics of the tested igneous rocks, a degradation ratio (RD) was calculated and applied to physical and mechanical properties, including bulk density (ρ_b), effective porosity (pe), ultrasound pulse velocity (Vp), and abrasion loss rate (Abr), using the following formula:

$$RD = \left(1 - \frac{Rn}{Ro}\right) \times 100 \quad (11)$$

Where Rn is the physico-mechanical parameters after 100 cycles, and Ro is the initial physico-mechanical properties before cyclic freezing thawing of the studied igneous rock samples. According to the results displayed in Table 5, the maximum increase in deterioration ratio (RD) of effective porosity is 6.3 % for monzonite specimens, while the minimum is 5.03 % for diorite samples. The results also show that the highest decrease in damage ratio of compressional wave velocity is 3.2% for rock specimens of monzonite, whereas the lowest is 1.4% for diorite specimens. In addition, the highest increase deterioration ratio of abrasion is 3.6 % for rock specimens of monzonite, while the lowest is 2.5 % for samples of diorite. According to the results of deterioration rate of bulk density displayed in Table 5, this parameter was virtually not influenced by cyclic freezing-thawing and there was no clear weight decrease. In fact, the deterioration ratio factor provides valuable information on the change trends of the rock characteristics against freezing thawing cycles, so the variations in the physico-mechanical properties including bulk density (ρ_b), effective porosity (p_e), ultrasound pulse velocity (V_p) and abrasion loss rate (Abr) are indicated in Figures. 3 a-d, respectively. As shown in Figures 3b-3d, the changes in effective porosity and abrasion rate show an increasing trend with increasing the cyclic freezing-thawing. An exponential model was found to be the best fit for changes in effective porosity, while the best fit for abrasion rate variations was a linear model. As presented in Figure 3b, it can be observed that the change in limits of effective porosity supports high durability of the tested igneous rocks under freezing-thawing cycles.

On the other hand, it can be noticed that the ultrasound pulse velocity changes exhibit a decreasing trend with increasing the number of cyclic freezing-thawing cycles (Figure 3c). The tested igneous rocks show indicate a critical loss of ultrasound pulse velocity in a linear model. Generally, the high values of coefficient of determination (R^2) of ultrasound pulse velocity and abrasion rate indicate that theses parameters are more sensitive to the influence of the freezing-thawing test and will be utilized as decay indicators. Inspecting the changes in bulk density reveals that the rate of decrease is very low, therefore this property is not sensitive to the cyclic freezing-thawing weathering influences (Figure 3a).

3.2. Assessment of rock strength properties using decay function model

For investigating the model's validity in predicting the rate of integrity decrease due to cyclic freezing-thawing weathering, laboratory tests of uniaxial compression and point load index were performed on igneous rock samples. The results of the mechanical strength properties, including uniaxial compression and point load index of igneous rocks subjected to freezing-thawing cycles, are presented in Table 6. As observed in this table, the changes in uniaxial compression and point load index strengths showed a decreasing trend with increasing freeze-thaw cycles. This indicates progressive micro-crack propagation along grain boundaries, with crack density increasing per cycle (qualitatively). It can also be observed that the maximum variations in uniaxial compression and point load values were for monzonite samples (MO), while the minimum variations were for rock specimens of granodiorite (GD). It is observed that at the end of 100 cycles, the monzonite specimens have the lowest values of uniaxial compression and point load strengths (70.94 MPa and 5.5 MPa, respectively). Therefore, the variation of strength properties shows a distinct manner of degradation between different rock samples. It can be said that the variation in uniaxial compressive and point load strength values is due to widening of preexisting micro-cracks and pores during cyclic freezing-thawing, which affects the mechanical properties of rock specimens [19]. Moreover, water in the capillary fractures and micro-pores of rocks leads to disintegration. The frozen fluid in the cavity will increase in volume by up to 9%, causing degradation [61], [62]. Mechanistically, diorite's superior durability results from its tightly interlocked texture and minimal initial micro-crack density, which limit water ingress and restrict ice-induced crack propagation despite the 9% volume expansion. In monzonite, higher initial porosity allows rapid crack widening, accelerating deterioration. When more pores or capillary cracks develop in the stones, deterioration accelerates and durability decreases, as can be seen in monzonite rock samples.

According to the results presented in Table 6, simple regression analysis models were used to determine the decay function model parameters such as the decay constant (λ) and the half-life ($N_{1/2}$). The authors attempted to develop the best correlation—linear, non-linear, exponential, or logarithmic regression models—between the mechanical strength properties of the tested igneous rocks and the freezing–thawing cycles to obtain the most reliable empirical equation. The equations of the best-fitted line, the 95% confidence limits, and the correlation coefficients (R^2) were obtained for each regression. Figures 4a–d show the changes in the mechanical strength properties of the tested rocks during the freezing–thawing cycles. In all cases, exponential regression equations were found to fit the data well, excluding the results of the point load index strength of granodiorite samples, which exhibited a linear regression trend. The degree of fit to this model could be evaluated by the values of determination coefficients (R^2), which measure the proportion of change in the dependent variable [63]. The high values of determination coefficients (R^2) facilitate the estimation of the mechanical properties of the tested igneous rocks after any freezing–thawing cycle (Table 7). Hence, the predictive power of the point load strength of the studied rocks ranges between 94.3% and 99.2%, and that for the unconfined compressive strength ranges from 97.3% to 99.6%. These values are statistically significant and close to 100%. It can be concluded that the integrity decrease parameters of rocks against freezing-thawing cycles correlate substantially with each other, and the studied model can be of practical use for estimating stone durability.

Table 5. average values and standard deviations of engineering properties of samples under F-T cycles.

Cyclic number	GR	GD	DI	MO
		ρ_b (g/cm^3)		
0	2.570±0.02	2.650±0.14	2.760±0.08	2.620 ±0.07
20	2.570±0.01	2.651±0.10	2.760±0.06	2.619±0.10
40	2.569±0.06	2.650±0.11	2.759±0.09	2.618±0.11
60	2.569±0.09	2.649±0.13	2.760±0.04	2.618±0.14
80	2.5688±0.11	2.648±0.09	2.759±0.06	2.6179±0.11
100	2.5690±0.08	2.648±0.10	2.759±0.05	2.6178±0.13
Deterioration ratio (DR%)	0.04	0.08	0.04	0.084
		p_e (%)		
0	0.90±0.66	0.86±0.52	0.79±0.50	1.12±0.80
20	0.91±0.78	0.85±0.95	0.77±0.72	1.13±0.85
40	0.92±0.44	0.86±0.94	0.80±0.81	1.12±0.86
60	0.94±0.41	0.87±0.88	0.81±0.67	1.15±0.92
80	0.93±0.56	0.875±1.12	0.811±0.70	1.14±0.96
100	0.95±0.88	0.91±1.01	0.83±0.78	1.19±0.90
Deterioration ratio (DR%)	5.6	5. 8	5.01	6.3
		Vp (km/s)		
0	4.64±0.33	4.84±0.87	5.64±0.72	4.02±0.98
20	4.62±0.30	4.83±0.80	5.63±0.76	3.99±0.90
40	4.58±0.40	4.81±0.86	5.62±0.90	3.99±0.77
60	4.56±0.50	4.82±0.70	5.60±0.89	3.96±0.68
80	4.54±0.60	4.78±0.77	5.61±0.59	3.94±0.96
100	4.53±0.55	4.72±0.90	5.56±0.70	3.89±0.94
Deterioration ratio (DR%)	2.4	2.3	1.4	3.2
		Abr (mm)		
0	0.150±0.33	0.140±0.44	0.100±0.66	0.190±0.60
20	0.151±0.40	0.140±0.37	0.100±0.85	0.192±0.77
40	0.152±0.50	0.141±0.50	0.1011±0.77	0.194±0.80
60	0.154±0.45	0.142±0.55	0.1022±0.90	0.195±0.70
80	0.154±0.70	0.142±0.40	0.1025±0.88	0.195±0.67
100	0.155±0.60	0.144±0.54	0.1025±0.81	0.197±0.74
Deterioration ratio (DR%)	3.3	2.9	2.5	3.6

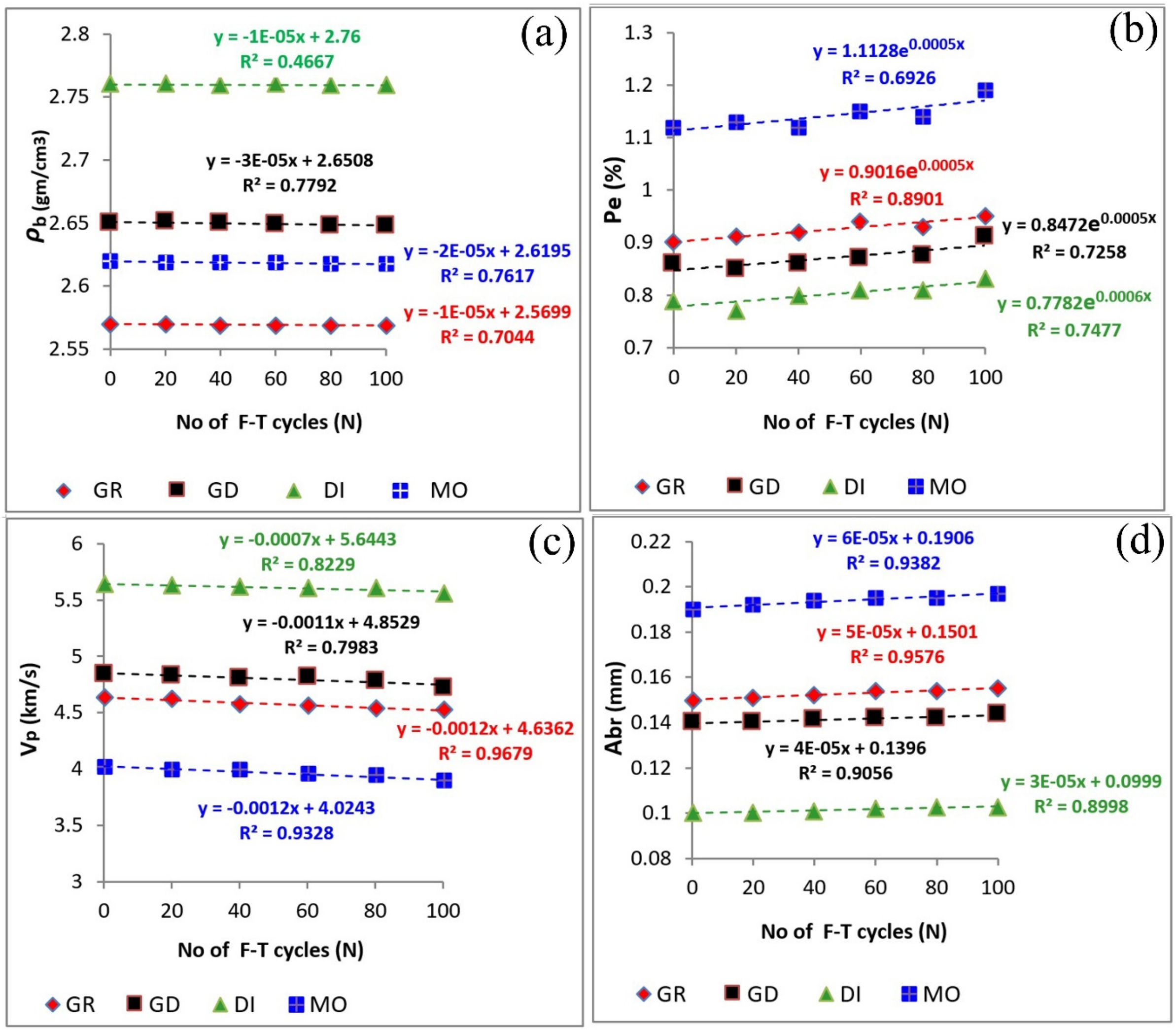

Figure 3. Variations in physico-mechanical properties of the studied igneous rocks under freeze–thaw (F-T) cycles: (a) Dry bulk density (ρ_b, g/cm³); (b) Porosity (pe, %); (c) Ultrasound pulse velocity (Vp, km/s); (d) Abrasion loss (Abr, mm).

Table 6. Mean values and standard deviations of UCS and IS of rocks against F-T cycles.

Cyclic number	GR	GD	DI	MO
		UCS (Mpa)		
0	117.32±1.84	132.95±1.31	162.21±1.83	99.97 ±1.89
20	114.57±1.81	130.40.±1.40	158.76±1.77	94.63±1.77
40	112.56±1.66	126.89±1.37	155.75±1.56	88.30±1.70
60	108.80±1.55	122.64±1.50	148.10±1.70	82.70±1.68
80	103.76±1.40	116.23 ±1.67	144.80±1.46	75.61±1.64
100	99.92±1.88	115.11±1.41	137.60±1.77	70.94±1.76
		IS (Mpa)		
0	8.04±0.75	8.96±0.32	10.12±0.60	7.12±0.37
20	7.66±0.78	8.80±0.85	9.85±0.76	6.70±0.85
40	7.46±0.44	8.70±0.94	9.45±0.85	6.33±0.86
60	7.30±0.48	8.55±0.88	9.16±0.67	6.12±0.90
80	7.21±0.59	8.10±0.78	8.88±0.70	5.73±0.94
100	7.08±0.80	7.92±0.65	8.75±0.77	5.50±0.90

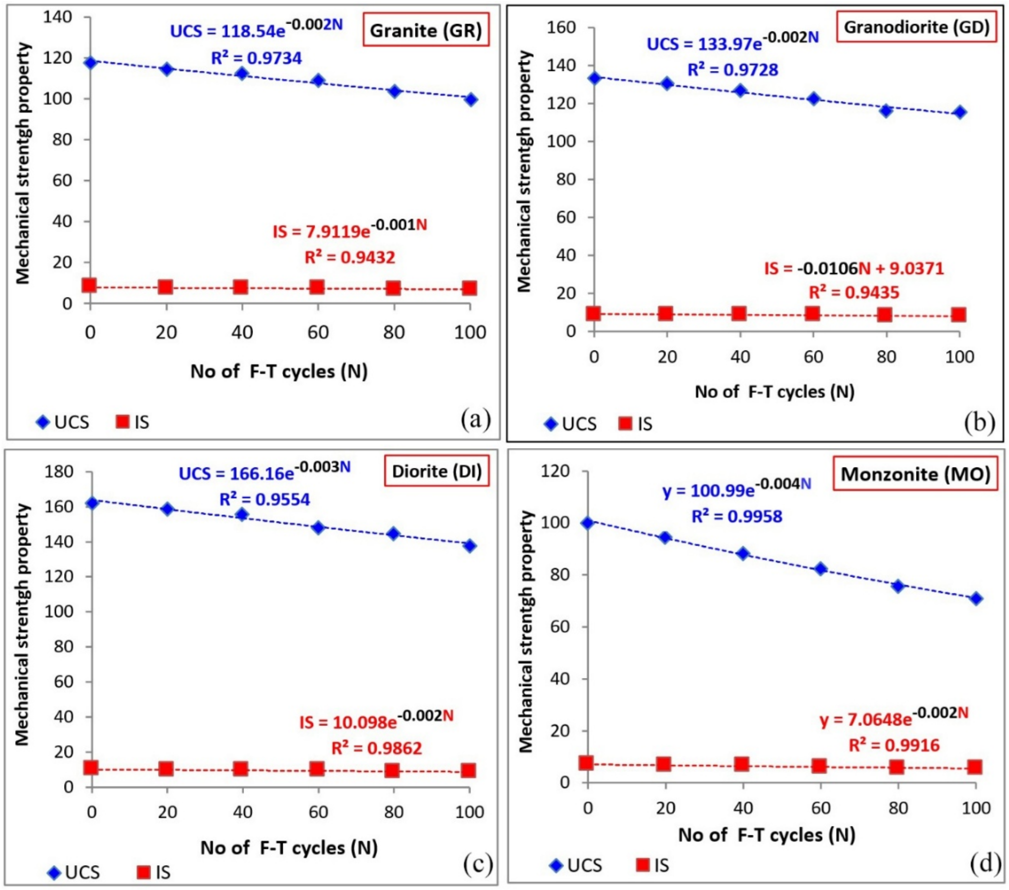

Figure 4. Changes in uniaxial compressive strength (UCS, MPa) and point load strength index (IS, MPa) under freeze–thaw (F-T) cycles for the four studied igneous rock types: (a) Granite; (b) Granodiorite; (c) Diorite; (d) Monzonite.

Table 7. Determination of R^2 values from the fitting curves of the regression models.

Uniaxial compressive strength (UCS)			
Rock type	**UCS(MPa)**	**Equation form**	**Model**
GR	0.9734	UCS = 118.54exp-0.002N	exponential
GD	0.9728	UCS = 133.97exp-0.002N	exponential
DI	0.9554	UCS = 166.16 exp-0.003N	exponential
MO	0.9958	UCS = 100.99 exp-0.004 N	exponential
Point load (IS)			
Rock type	**IS (Mpa)**	**Equation form**	**Model**
GR	0.9432	IS = 7.9119 exp-0.001N	exponential
GD	0.9435	IS = -0.0106N + 9.0371	linear
DI	0.9862	IS = 10.098exp-0.002N	exponential
MO	0.9916	IS= 7.0648exp-0.002N	exponential

3.2.1. Decay constant and half-life

The decay function models, including exponential and linear regression analyses, have been postulated and verified by experimental work. The decay function models provide two parameters, including the decay constant (λ) and half-life ($N_{1/2}$), to estimate the rate of integrity loss of the mechanical properties and, therefore, the rocks' durability under the freezing–thawing process. The decay constant (λ) values for unconfined compressive and point load index strengths of the tested rocks are presented in Table 8. As shown in this table, the studied igneous rock specimens have comparable decay constant values, indicating the model's usability and validity for rock strength properties. However, the decay constant values for uniaxial compressive strength are higher than those for the point load strength of the specimens, which suggests that the uniaxial compression test is more sensitive to cyclic freezing–thawing compared to the point load index. This can be attributed to the fact that igneous rocks of a similar type provide significant information about their durability against cyclic freezing–thawing. For instance, as observed in Table 8, some of the maximum durable igneous specimens (GR) and (GD), as well as one of the minimum durable samples (MO), exhibit the effects of the freezing–thawing process (i.e., indicating the minimum and maximum decay constant values of uniaxial compressive strength, λ = −0.002 and −0.004, respectively). These specimens are of a comparable rock type. In fact, the MO igneous specimens decrease only 0.4% of their initial uniaxial compressive strength value, on average, after one freezing–thawing cycle, while the GR samples lose 0.2%. Therefore, the integrity loss rate of MO igneous specimens is twice that of the GR and GD specimens. On the other hand, the half-life values ($N_{1/2}$) for the decrease of unconfined compressive and point load strengths of igneous specimens under cyclic freezing–thawing weathering are listed in Table 9 and graphically displayed in Figures 5a–b, respectively. It is observed that the half-life values based on uniaxial compression strength are lower than those based on point load strength. Since decay constant and half-life values are inversely related, their evolution, derived from the studied model, should be comparable. Therefore, the half-life parameter obtained from uniaxial compressive and point load tests can be used to assess the durability of the studied rocks against cyclic freezing–thawing. It is also noted that rocks exhibiting high resistance to deterioration induced by cyclic freezing–thawing have higher half-life values and are thus more durable. Based on these results, the tested samples demonstrated high resistance to disintegration caused by cyclic freezing–thawing. In general, the tested rocks can be used as construction and decorative stones in cold environments over long periods without deterioration, except for the monzonite (MO) samples.

Table 8. Decay constant values under cyclic F-T.

	Decay constant (λ)	
Rock type	**UCS (MPa)**	**IS (Mpa)**
GR	-0.002	-0.001
GD	-0.002	-0.0106
DI	-0.003	-0.002
MO	-0.004	-0.002

Table 9. Half-life values under cyclic F-T.

	Half-life ($N_{1/2}$)	
Rock type	**UCS (MPa)**	**IS (Mpa)**
GR	364.5	693.0
GD	364.5	423.0
DI	231.0	346.5
MO	173.25	346.5

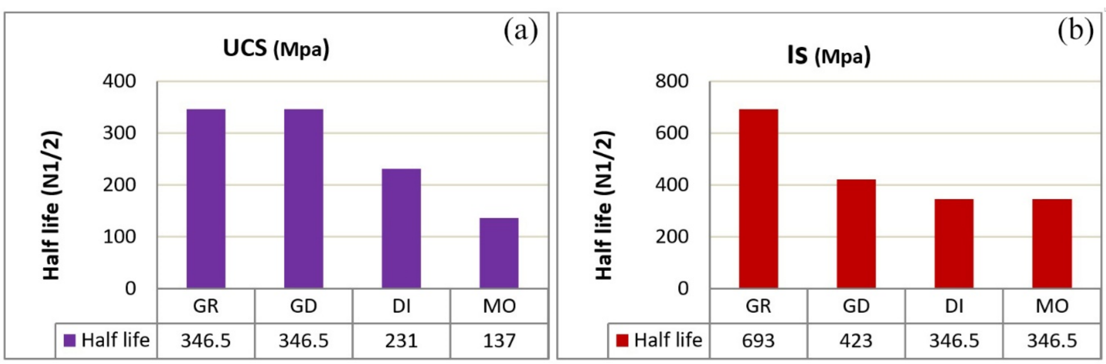

Figure 5. (a) Half-life values of UCS against F-T cycles and (b) Half-life values of IS against F-T cycles.

4. Conclusions and Recommendations

To study the rock degradation caused by the repeated cyclic freezing-thawing weathering process, the physico-mechanical properties of four types of Egyptian igneous rocks used as construction and ornamental stones were tested before and after 20, 40, 60, 80, and 100 cycles of the freezing-thawing process. The long-term durability of the tested rocks was evaluated using the loss of integrity in some of the physico-mechanical properties during these tests, as well as their decay constant (λ) and half-life ($N_{1/2}$) parameters obtained from decay function models. The following major conclusions can be drawn from the present study:

- Exponential and linear decay function models were established for estimating the integrity loss of the mechanical strength parameters of the studied igneous rocks subjected to cyclic freezing-thawing weathering. The models demonstrated the susceptibility of the tested rock samples to cyclic freezing-thawing action. The decay constant and half-life values of the mechanical strength parameters across different rocks are highly comparable and show strong correlation. Therefore, these models and the extracted parameters are highly precise and can be used to estimate the integrity loss characteristics of the studied rocks. Moreover, these models are reliable for rocks extracted from approximately the same areas and with comparable characteristics.
- Low effective porosity and high strength play a vital role in the resistance of the tested igneous rocks to deterioration induced by repeated freezing-thawing weathering. Therefore, these rocks can be used for decorative purposes in cold environments; however, caution should be taken for monzonite samples.
- Ultrasound pulse velocity is more sensitive to rock decay due to the physical aging process; hence, this parameter is the best physical indicator of repeated freezing-thawing action, whilst unconfined compression is the best mechanical indicator for evaluating the influence of repeated freezing-thawing on rock properties.
- Inspection of the variations in dry bulk density shows that the decrease rate is very low and there is no significant weight loss; therefore, this property is not sensitive to cyclic freezing-thawing weathering effects.

Based on the results obtained from the present study, the tested igneous rocks may be suitable for use in regions subject to repeated freezing-thawing effects. However, future studies need to apply the freezing-thawing weathering process to rocks of different origins to obtain a more complete assessment of rock damage. The studied models can be used to predict the integrity loss characteristics and/or durability of rocks. However, future research needs to use other statistical models with various types of rocks and compare the results from these models.

Future studies should apply more than 100 cycles of freeze–thaw on similarly hard, low-porosity igneous rocks (e.g., granite and granodiorite) in order to obtain more robust half-life estimates from the decay function model, better constrain long-term degradation trends and incorporate long-term climate trend analysis in addition link predicted half-life cycles to actual annual freeze–thaw frequency in the field. Therefore, these efforts will further constrain degradation time scales and strengthen the connection between laboratory experiments and natural environmental conditions.

References

[1]. Rashwan, M. A., Lasheen, E. S. R., & Azer, M. K. (2023). Thermal and physico-mechanical evaluation of some magmatic rocks at Homrit Waggat Area, Eastern Desert, Egypt: petrography and geochemistry. *Bulletin of Engineering Geology and the Environment*, *82*.

[2]. Khaleal, F. M., Lentz, D. R., Kamar, M. S., Saleh, G. M., & Lasheen, E. S. R. (2023). Critical raw material resources in Nugrus-Sikait area, South Eastern Desert, Egypt: Geological and geochemical aspects. *Journal of African Earth Sciences*, *197*.

[3]. Saleh, G. M., Kamar, M. S., Lasheen, E. S. R., Ibrahim, I. H., & Azer, M. K. (2022). Whole rock and mineral chemistry of the rare metals-bearing mylonitic rocks, Abu Rusheid borehole, south Eastern Desert, Egypt. *Journal of African Earth Sciences*, *196*.

[4]. Azer, M. K., Abdelfadil, K. M., Asimow, P. D., & Khalil, A. E. (2020). Tracking the transition from subduction-related to post-collisional magmatism in the north Arabian–Nubian Shield: A case study from the Homrit Waggat area of the Eastern Desert of Egypt. *Geological Journal*, *55*(6), 4426-4452.

[5]. Lasheen, E. S. R., Azer, M. K., Ene, A., Abdelwahab, W., Zakaly, H. M. H., Awad, H. A., & Kawady, N. A. (2022). Radiological Hazards and Natural Radionuclide Distribution in Granitic Rocks of Homrit Waggat Area, Central Eastern Desert, Egypt. *Materials*, *15*.

[6]. Abdel-Karim, A. A., Azer, M., & Sami, M. (2021). Petrogenesis and tectonic implications of the Maladob ring complex in the South Eastern Desert, Egypt: new insights from mineral chemistry and whole-rock geochemistry. *International Journal of Earth Sciences*, *110*(1), 53-80.

[7]. Mashaly, A. O., El-Kaliouby, B. A., Shalaby, B. N., El-Gohary, A. M., & Rashwan, M. A. (2016). Effects of marble sludge incorporation on the properties of cement composites and concrete paving blocks. *Journal of Cleaner Production*, *112*, 731-741.

[8]. Abdelhamid, M. M. A., & Mousa, B. G. (2023). A prediction method for abrasion loss rate of some Egyptian carbonate rocks due to cyclic salt crystallization weathering using physico-mechanical deterioration: insights from laboratory investigations. *Acta Geodaetica et Geophysica*, *58*(1), 53-70.

[9]. Embaby, A., Ismael, A., Ali, F. A., Farag, H. A., Mousa, B. G., Gomaa, S., & Elwageeh, M. (2023). An

approach based on Machine Learning Algorithms, Geostatistical Technique, and GIS analysis to estimate phosphate ore grade at the Abu Tartur Mine, Western Desert, Egypt. *Mining of Mineral Deposit*, 17, 108-119..

[10]. Abdelhamid, M. M. A., Mousa, B. G., Waqas, H., Elkotb, M. A., Eldin, S. M., Munir, I., Ali, R., & Galal, A. M. (2022). Artificial Thermal Quenching and Salt Crystallization Weathering Processes for the Assessment of Long-Term Degradation Characteristics of Some Sedimentary Rocks, Egypt. *Minerals, 1393*, *12*(11).

[11]. Fort, R., Alvarez de Buergo, M., & Perez-Monserrat, E. M. (2013). Non-destructive testing for the assessment of granite decay in heritage structures compared to quarry stone. *International Journal of Rock Mechanics and Mining Sciences*, *61*, 296-305.

[12]. Alzahrani, A. M., Lasheen, E. S. R., & Rashwan, M. A. (2022). Relationship of Mineralogical Composition to Thermal Expansion, Spectral Reflectance, and Physico-Mechanical Aspects of Commercial Ornamental Granitic Rocks. *Materials ,2041*, *15*(6).

[13]. Lasheen, E. S. R., Rashwan, M. A., & Azer, M. K. (2023). Effect of mineralogical variations on physico-mechanical and thermal properties of granitic rocks. *Scientific Reports*, *13*.

[14]. Rashwan, M. A., Lasheen, E. S. R., Abdelwahab, W., Azer, M. K., Zakaly, H. M. H., Alarifi, S. S., Ene, A., & Thabet, I. A. (2023). Physico-mechanical properties and shielding efficiency in relation to mineralogical and geochemical compositions of Um Had granitoid, Central Eastern Desert, Egypt. *Frontiers in Earth Science*, *11*.

[15]. Fraská, M., & Yamamoto, J. (2006). Ageing tests for dimension stone - experimental studies of granitic rocks from Brazil. *IAEG (Geological Society of London)*(224), 1-9.

[16]. Yavuz, H., Altindag, R., Sarac, S., Ugur, I., & Sengun, N. (2006). Estimating the index properties of deteriorated carbonate rocks due to freeze-thaw and thermal shock weathering. *International Journal of Rock Mechanics and Mining Sciences*, *43*, 767-775.

[17]. Yavuz, A. B., Akal, C., Türk, N., Çolak, M., & Tanyu, B. F. (2015). Investigation of discrepancy between tuff used as building stones in historical and modern buildings in western Turkey. *Construction and Building Materials*, *93*, 439-448.

[18]. Tuğrul, A. (2004). The effect of weathering on pore geometry and compressive strength of selected rock types from Turkey. *Engineering Geology*, *75*, 215-227.

[19]. Chen, T. C., Yeung, M. R., & Mori, N. (2004). Effect of water saturation on deterioration of welded tuff due to freeze-thaw action. *Cold Regions Science and Technology*, *38*(2-3), 127-136.

[20]. Takarli, M., Prince, W., & Siddique, R. (2008). Damage in granite under heating/cooling cycles and water freeze-thaw condition. *International Journal of Rock Mechanics and Mining Sciences*, *45*, 1164-1175.

[21]. Wang, Y., Feng, W. K., Wang, H. J., Li, C. H., & Hou, Z. Q. (2020). Rock bridge fracturing characteristics in granite induced by freeze-thaw and uniaxial deformation revealed by AE monitoring and post-test CT scanning. *Cold Regions Science and Technology*, *177*.

[22]. Wang, Y., Zhang, B., Gao, S. H., & Li, C. H. (2021). Investigation on the effect of freeze-thaw on fracture mode classification in marble subjected to multi-level cyclic loads. *Theoretical and Applied Fracture Mechanics*, *111*.

[23]. Zhang, J., Deng, H., Taheri, A., Ke, B., & Liu, C. (2019). Deterioration and strain energy development of sandstones under quasi-static and dynamic loading after freeze-thaw cycles. *Cold Regions Science and Technology*, *160*, 252-264.

[24]. Zhang, H., Meng, X., & Yang, G. (2020). A study on mechanical properties and damage model of rock subjected to freeze-thaw cycles and confining pressure. *Cold Regions Science and Technology*, *174*, 103056.

[25]. Ruedrich, J., Kirchner, D., & Siegesmund, S. (2011). Physical weathering of building stones induced by freeze-thaw action: A laboratory long-term study. *Environmental Earth Sciences*, *63*, 1573-1586.

[26]. Martínez-Martínez, J., Benavente, D., Gomez-Heras, M., Marco-Castaño, L., & García-Del-Cura, M. Á. (2013). Non-linear decay of building stones during freeze-thaw weathering processes. *Construction and Building Materials*, *38*, 443-454.

[27]. Bayram, F. (2012). Predicting mechanical strength loss of natural stones after freeze–thaw in cold regions. *Cold Regions Science and Technology*, *83-84*, 98-102.

[28]. Sarici, D. E., & Ozdemir, E. (2018). Determining point load strength loss from porosity, Schmidt hardness, and weight of some sedimentary rocks under freeze–thaw conditions. *Environmental Earth Sciences*, *77*.

[29]. Seyed Mousavi, S. Z., Tavakoli, H., Moarefvand, P., & Rezaei, M. (2019). Assessing the effect of freezing-thawing cycles on the results of the triaxial compressive strength test for calc-schist rock. *International Journal of Rock Mechanics and Mining Sciences*, *123*.

[30]. Mousavi, S. Z. S., Tavakoli, H., Moarefvand, P., & Rezaei, M. (2020). Micro-structural, petro-graphical and mechanical studies of schist rocks under the freezing-thawing cycles. *Cold Regions Science and Technology*, *174*.

[31]. Rezaei, Seyed Zanyar Seyed Mousavi, Hossein

Tavakoli, Parviz Moarefvand, M. (2020). Evaluating the variations of density and durability index of schist rock under the effect of freezing-thawing cycles. Iranian Sociecty of Mining Engineering , *45*, 1-12.

[32]. Mousavi, S. Z. S., & Rezaei, M. (2022). Correlation assessment between degradation ratios of UCS and non-destructive properties of rock under freezing-thawing cycles. *Geoderma*, *428*.

[33]. Mousavi, S. Z. S., & Rezaei, M. (2023). Assessing the long-term durability and degradation of rocks under freezing-thawing cycles. *Geomechanics and Engineering*, *34*, 51-67.

[34]. Mutlutürk, M., Altindag, R., & Türk, G. (2004). A decay function model for the integrity loss of rock when subjected to recurrent cycles of freezing-thawing and heating-cooling. *International Journal of Rock Mechanics and Mining Sciences*, *41*, 237-244.

[35]. Yavuz, H. (2011). Effect of freeze-thaw and thermal shock weathering on the physical and mechanical properties of an andesite stone. *Bulletin of Engineering Geology and the Environment*, *70*, 187-192.

[36]. Tan, X., Chen Weizhong, W., Yang, J., & Cao, J. (2011). Laboratory investigations on the mechanical properties degradation of granite under freeze-thaw cycles. *Cold Regions Science and Technology*, *68*, 130-138.

[37]. Hua, L., Fu-Jun, N., Zhi-Ying, X., Zhan-Ju, L., & Jian, X. (2011). *Acoustic experimental study of two types of rock from the Tibetan Plateau under the condition of freeze-thaw cycles*. China Science Publishing & Media Ltd.

[38]. Özbek, A. (2014). Investigation of the effects of wetting-drying and freezing-thawing cycles on some physical and mechanical properties of selected ignimbrites. *Bulletin of Engineering Geology and the Environment*, *73*, 595-609.

[39]. Jamshidi, A., Nikudel, M. R., & Khamehchiyan, M. (2013). Predicting the long-term durability of building stones against freeze-thaw using a decay function model. *Cold Regions Science and Technology*, *92*, 29-36.

[40]. Jamshidi, A., Nikudel, M. R., & Khamehchiyan, M. (2016). Evaluation of the durability of Gerdoee travertine after freeze–thaw cycles in fresh water and sodium sulfate solution by decay function models. *Engineering Geology*, *202*, 36-43.

[41]. Momeni, A., Abdilor, Y., Khanlari, G. R., Heidari, M., & Sepahi, A. A. (2016). The effect of freeze–thaw cycles on physical and mechanical properties of granitoid hard rocks. *Bulletin of Engineering Geology and the Environment*, *75*, 1649-1656.

[42]. Zhang, J., Deng, H., Taheri, A., Ke, B., Liu, C., & Yang, X. (2018). Degradation of physical and mechanical properties of sandstone subjected to freeze-thaw cycles and chemical erosion. *Cold Regions Science and Technology*, *155*, 37-46.

[43]. Ma, Z. jing, Zhang, Z. jian, Li, B., & Liu, J. bin (2019). Effects of rain and heat-cool cycles on the weathering behavior of basalt from Wudalianchi, Heilongjiang Province, NE China. *Bulletin of Engineering Geology and the Environment*, *78*, 6033-6045.

[44]. Fan, L., Xu, C., & Wu, Z. (2020). Effects of cyclic freezing and thawing on the mechanical behavior of dried and saturated sandstone. *Bulletin of Engineering Geology and the Environment*, *79*, 755-765.

[45]. Chen, D., Li, G., Li, J., Du, Q., Zhou, Y., Mao, Y., Qi, S., Tang, L., Jia, H., & Peng, W. (2023). Mechanical characteristics and damage evolution of granite under freeze–thaw cycles. *Frontiers in Energy Research*, *10*, 983705.

[46]. Yun, M., Ren, J., Song, Y., Zhang, L., Sun, C., Chang, P., & Cao, X. (2024). Fracture Mechanism and Damage Constitutive Model of Freeze–Thaw Fissured Granite Subjected to Fatigue Loading. *Applied Sciences , 6324*, *14*(14).

[47]. Omran, E.-S. E., & Negm, A. M. (2020). Egypt's Environment from Satellite. pp. 23-91.

[48]. Jamshidi, A., Nikudel, M. R., & Khamehchiyan, M. (2013). Predicting the long-term durability of building stones against freeze–thaw using a decay function model. *Cold Regions Science and Technology*, *92*, 29-36.

[49]. Kock, T. De, Turmel, A., Fronteau, G., & Cnudde, V. (2017). Rock fabric heterogeneity and its influence on the petrophysical properties of a building limestone: Lede stone (Belgium) as an example. *Engineering Geology*, *216*, 31-41.

[50]. Brown.E.T *ISRM (1981) Suggested Method for Rock Characterization, Testing and Monitoring, ISRM Commission on Testing Methods. Pergamon Press, Oxford.*.

[51]. Martínez-Martínez, J., Benavente, D., & García-del-Cura, M. A. (2011). Spatial attenuation: The most sensitive ultrasonic parameter for detecting petrographic features and decay processes in carbonate rocks. *Engineering Geology*, *119*, 84-95.

[52]. Diamantis, K., Gartzos, E., & Migiros, G. (2009). Study on uniaxial compressive strength, point load strength index, dynamic and physical properties of serpentinites from Central Greece: Test results and empirical relations. *Engineering Geology*, *108*, 199-207.

[53]. Franklin, J. A. (1985). Suggested method for determining point load strength. *International Journal of Rock Mechanics and Mining Sciences and*, *22*, 51-60.

[54]. BS EN 14157:2017-TC: Natural stone test

methods. Determination of the abrasion resistance (2017).

[55]. HUDSON, R. U. & J. A. (2007). *The Complete ISRM Suggested Methods for Rock Characterization, Testing and Monitoring; 1974-2006*. Kozan Ofset Matbaacılık San. ve Tic. Şti. Büyük Sanayi 1. Cadde, No. 95/22, İskitler Ankara, Turkey.

[56]. Egyptian code . https://www.eos.org.eg/ar

[57]. ASTM International (2013). B611 - Standard Test Method for Determining the High Stress Abrasion Resistance of Hard Materials. , 1-6.

[58]. Wang, J., Cui, D., Chen, Q., Chen, J., & Dai, M. (2025). Morphological damage and strength deterioration of red sandstone under freeze–thaw cycles. *Journal of Rock Mechanics and Geotechnical Engineering*, *17*, 671-687.

[59]. Brown. E. T. *Rock Characterisation,Testing and Monitoring. Pergamon Press,Oxford*.

[60]. Blair, B. E. (1995). *Physical properties of mine rocks.Part III.*. United States Department of the Interio.

[61]. Weng, L., Wu, Z., Taheri, A., Liu, Q., & Lu, H. (2020). Deterioration of dynamic mechanical properties of granite due to freeze-thaw weathering: Considering the effects of moisture conditions. *Cold Regions Science and Technology*, *176*.

[62]. Johnson, R. A., & Wichern, D. W. (20002). *Applied multivariate statistical analysis* (5th ed.). Prentice Hall, Upper Saddle River.

[63]. Bell, F. G. (1993). Durability of carbonate rock as building stone with comments on its preservation. *Environmental Geology*, *21*(4), 187-200.

انجمن مهندسی معدن ایران
نشریه مهندسی معدن و محیط زیست
نشانی نشریه: www.jme.shahroodut.ac.ir
دانشگاه صنعتی شاهرود

ارزیابی ویژگی‌های سنگ و تخریب ناشی از عمل انجماد-ذوب چرخه‌ای برخی از سنگ‌های آذرین تحت شرایط تغییر آب و هوا در منطقه کوهستانی خشک سنت کاترین، جنوب سینا، مصر

ی. جی. موسی[۱،۲*]، مرزوق محمد علی عبدالحمید[۲]، محمد الغریب گوماه[۲]، ام. ام. زکی۲، اچ. ای. فراگ[۲]، دبلیو. ام. دراز[۲]، رموندا دامیان[۱،۳،۴]، و یوسف ای. المسنی[۱،۳]

۱ .آزمایشگاه کلیدی دولتی ایمنی اکولوژیکی و توسعه پایدار در مناطق خشک، موسسه اکولوژی و جغرافیای سین کیانگ، آکادمی علوم چین، ارومچی ۸۳۰۰۱۱، چین

۲ .گروه مهندسی معدن و نفت، دانشکده مهندسی، دانشگاه الازهر، قاهره ۱۱۸۸۴، مصر

۳ .دانشگاه آکادمی علوم چین، پکن ۱۰۰۰۴۹، چین

۴. گروه خاک و استفاده از آب، موسسه تحقیقات کشاورزی و بیولوژیکی، مرکز تحقیقات ملی، قاهره، ۱۲۶۲۲، مصر

اطلاعات مقاله

تاریخ ارسال: ۲۰۲۶/۰۲/۰۶

تاریخ داوری: ۲۰۲۶/۰۵/۳۰

تاریخ پذیرش: ۲۰۲۶/۰۶/۳۱

DOI: 10.22044/jme.2026.17427.3461

کلمات کلیدی

سنگ‌های آذرین

هوازدگی فیزیکی

انجماد-ذوب

مدل تابع زوال

دوام طولانی مدت

چکیده

آسیب سنگ به دلیل شرایط سخت محیطی ممکن است در طول زمان بر دوام آن تأثیر بگذارد. بنابراین، این مطالعه با هدف بررسی تخریب سنگ‌های آذرین ناشی از هوازدگی انجماد-ذوب و پیش‌بینی از دست دادن یکپارچگی آنها انجام شده است. چهار نوع سنگ آذرین از منطقه کوهستانی سنت کاترین، سینا، مصر جمع‌آوری و تحت ۱۰۰ چرخه روش انجماد-ذوب قرار گرفتند. تغییرات دمای سطح زمین با استفاده از داده‌های سنجش از دور به عنوان شاخصی برای انتخاب دمای انجماد-ذوب برای آزمایش‌های ما تجزیه و تحلیل شد. ویژگی‌های فیزیکی و مکانیکی سنگ‌های مورد مطالعه، مانند چگالی حجمی خشک، تخلخل مؤثر، سرعت پالس فراصوت، افت سایش، مقاومت فشاری آزاد و مقاومت بار نقطه‌ای، پس از ۰، ۲۰، ۴۰، ۶۰، ۸۰ و ۱۰۰ چرخه فرآیند انجماد-ذوب اندازه‌گیری و با استفاده از نسبت‌های زوال و مدل‌های آماری ارزیابی شدند. مدل‌های تابع واپاشی نمایی و خطی برای ارزیابی آماری نرخ از دست دادن یکپارچگی خواص مقاومت مکانیکی سنگ‌های انتخاب شده ایجاد شدند. دو عامل حیاتی، ثابت واپاشی و نیمه‌عمر، از مدل‌های مورد مطالعه استخراج و برای پیش‌بینی دوام سنگ استفاده شدند. این ارزیابی نشان می‌دهد که رفتار واپاشی سنگ در انواع مختلف سنگ‌های آذرین بسیار مشابه است و همبستگی قوی و دقت بالایی را نشان می‌دهد. بنابراین، این مدل‌ها برای پیش‌بینی دوام سنگ‌های آذرین مورد مطالعه قابل اعتماد و معتبر هستند. نتایج همچنین نشان داد که سنگ‌های آذرین آزمایش شده را می‌توان به عنوان سنگ‌های ساختمانی در مناطقی که در معرض هوازدگی چرخه‌ای مکرر انجماد-ذوب و شرایط سخت محیطی در دوره‌های طولانی بدون فروپاشی قرار دارند، استفاده کرد.

نویسنده مسئول مکاتبات: *dr.bahaa1@azhar.edu.eg* (ی.ج. موسی)